Testing Homeostasis Using the Designed Matlab GUI of Cardiovascular-Respiratory System Mathematical Model

E. Nyirishema ^{1*}, K. Ngarmadji ², J. M. Ntaganda ¹

- 1. University of Rwanda, College of Science and Technology, School of Science, Department of Mathematics.
- 2. Département de Mathématiques Informatique, Ecole Normale Supérieure de N'Djamena, Chad.
- * Corresponding author: nyirishema2017@gmail.com

Article Info

Received: 23 February 2025 Revised: 11 August 2025

Accepted: 15 August 2025 Available online: 31 August 2025

Abstract

Homeostasis is the body's mechanism for maintaining internal stability amidst external changes, particularly within the cardiovascular and respiratory systems. This study applied optimal control problem strategies to sustain homeostasis by regulating key physiological parameters such as blood pressure, oxygen, and carbon dioxide levels. A stability analysis was conducted on a mathematical model of the human cardiovascular-respiratory system using a GUI in MATLAB App Designer to test this homeostasis. The findings demonstrated that the model's variables consistently averaged within normal physiological ranges, affirming the successful maintenance of homeostasis. The GUI provided intuitive and interactive graphical outputs, effectively distinguishing between healthy and unhealthy individuals. Stable outputs were observed in healthy subjects, while instability was evident in unhealthy subjects, underscoring the system's sensitivity to pathological conditions. The user-friendly interface efficiently managed input data and delivered precise health status indicators. The model reliably simulated the impact of various disease parameters, with variables remaining within normal ranges in healthy scenarios and deviating in the presence of disease, thereby highlighting its potential as a valuable tool for clinical and research applications.

Keywords: Cardiovascular and Respirator System, Graphical User Interface, Homeostasis, Mathematical Model, MATLAB, Optimal Control Problem, Stability Analysis.

MSC2010: 92C30, 34A34, 65L05.

1 Introduction

A significant contemporary challenge is the rise in non-communicable chronic illnesses. It is crucial to implement measures to mitigate contributing factors to these diseases and improve overall population well-being. Such ailments predominantly affect the respiratory and cardiovascular systems. Homeostasis is maintained through various physiological mechanisms, including feedback systems that detect deviations and initiate corrective responses [1]. In the context of cardiovascular and respiratory systems, homeostasis refers to the body's ability to maintain stable internal conditions,



HTTPS://DOI.ORG/10.5281/ZENODO.17584815

such as blood pressure and oxygen levels, despite external changes [2]. Maintaining stability in these systems is essential for homeostasis, as it involves regulating physiological parameters like blood pressure, oxygen, and carbon dioxide levels to ensure proper bodily function and balance [3].

The graphical user interface (GUI) offers a user-friendly experience but presents challenges in design complexity. While it provides an intuitive user experience, advanced skills are required for effective design implementation. MATLAB, a widely-used software, excels at solving numerical problems but has limited resources for developing GUIs, which are advantageous for various applications [4]. GUIs offer an interactive and accessible approach to handling complex mathematical models and data, and are frequently employed in mathematical modeling and scientific applications [5]. GUI-based applications facilitate collaboration among researchers by offering a common platform where multiple users can work on and share mathematical models and their results [6]. Modern GUIs incorporate advanced features like drag-and-drop functionality, real-time feedback, and customizable interfaces, enhancing usability and productivity [7]. Additionally, GUIs support accessibility tools, such as screen readers and magnifiers, ensuring inclusivity for users with disabilities. As technology advances, GUIs continue to play a crucial role in human-computer interaction, with ongoing developments in virtual and augmented reality promising even more immersive and interactive experiences [8]. GUIs remain essential in bridging the gap between humans and machines, making complex systems more accessible and efficient. For instance, a standalone MATLAB application called CVSim has been utilized for teaching and research on cardiovascular and respiratory diseases [9]. MATLAB is used to analyze cardio-respiratory variability by processing physiological signals such as heart and respiratory rates [10].

Mathematical modeling of the cardiovascular-respiratory system is a complex process that captures the intricate interactions between the heart, blood vessels, and lungs [11]. These models integrate principles from fluid dynamics to describe blood flow, pressure-volume relationships to understand the mechanical properties of the heart and vessels, and gas exchange processes to account for the transfer of oxygen and carbon dioxide between the lungs and bloodstream. By doing so, they provide a detailed and dynamic representation of the cardiovascular and respiratory systems, allowing for the prediction of responses under different scenarios and aiding in the development of treatments and interventions [12]. A comprehensive model for the cardiovascular and respiratory system can be found in [13].

The design and implementation of GUIs for mathematical models, especially those concerning the cardiovascular-respiratory system, have garnered significant attention in recent research. For instance, [14] focused on creating a comprehensive GUI framework for simulating cardiorespiratory interactions in health and disease. These studies highlight the importance of GUIs in advancing the accessibility, usability, and applicability of mathematical models in understanding and managing cardiovascular-respiratory health.

In literature, MATLAB has been used independently for cardiovascular respiratory disease research, [16], [17], [18]. Additionally, a designed GUI in MATLAB have been employed as research tools in this field. Despite extensive study of the mathematical models of the cardiovascularrespiratory system, obtaining accurate information remains a significant challenge. The gap that must be tackled is the integration of MATLAB GUI used to test homeostasis, this facilitates realtime adjustments and stability analyses of the mathematical model, enabling researchers to effectively monitor and understand dynamic physiological responses and maintain system balance.

The goal of this paper is to study stability analysis of a mathematical model of a human cardiovascular-respiratory system to test homeostasis Using a graphical user interface (GUI) within MATLAB's App Designer to interact with a developed mathematical model of the cardiovascular and respiratory system [19].

In this paper, first, we focus on essential tools and theoretical frameworks for constructing a GUI using the mathematical model of the cardiovascular-respiratory system developed in [19], starting with an overview of MATLAB's functionalities. Secondly, the study of stability in nonlinear cardiovascular-respiratory system models begins with linearization, which simplifies analysis by approximating nonlinear systems near equilibrium points with linear systems. Finally, we formulate optimal control strategies based on this mathematical model to regulate the cardiovascularInternational Journal of Mathematical Sciences and Optimization: Theory and Applications 11(3), 2025, Pages 49 - 67

HTTPS://DOI.ORG/10.5281/ZENODO.17584815

respiratory system and maintain homeostasis.

This paper is structured as follow: section one focus on the introduction, section two comprises model presentation and stability analysis of mathematical model, section three focus formulation of optimal control for testing homeostasis of CRS (cardiovascular-respiratory system), section four deals with GUI design in MATLAB using mathematical model and present the results, section five focus discussion, and Conclusion of the study are finally drawn in section six.

2 Methods

2.1 Data

The data are utilized in the GUI input to determine the GUI output and estimate model parameters. These secondary data pertain to the cardiovascular respiratory system and were collected in [14], within the Rwandan context. They were employed to evaluate the Interface of the Cardiovascular Respiratory System Mathematical Model (ICRSMM), specifically through numerical tests for both normal and abnormal patients. Typically, numerical tests for abnormal subjects reveal elevated values in the cardiovascular-respiratory system. These results are influenced by the initial measurements provided by the user and entered into GUI, which are essential for calculating the parameters of the cardiovascular-respiratory system using a mathematical model governed by ordinary differential equations.

To validate the GUI's performance, we simulated physiological responses using a global mathematical model of the cardiovascular-respiratory system, originally developed by Timischl in [13]. The model was implemented in MATLAB and solved using its built-in ODE solver for both healthy and abnormal profiles. The simulated results served as benchmarks to assess the accuracy, consistency, and reliability of the GUI outputs. Finally, all results from the GUI were cross-verified with Timischl's model outputs to ensure alignment with established computational standards.

2.2 Mathematical model

Here, we present a nonlinear dynamic model that investigates the interaction between the respiratory and cardiovascular systems. With an emphasis on how well it applies to human physiology, this model has been carefully developed in [19].

The proposed model consists of four compartments of the cardiovascular-respiratory system (Pressures of systemic arterial (P_{as}) , systemic venous (P_{vs}) , oxygen-related area within arteries (P_{ao_2}) , and carbon dioxide-related area within arteries (P_{aco_2})) and two tissue compartments (venous concentrations of carbon dioxide (C_{vco_2}) and oxygen (C_{vo_2})). The heart and lungs maintain the body's oxygen and carbon dioxide levels, with exchange occurring in the lungs' alveoli and between systemic arteries and veins. The model includes parameters such as heart rate and alveolar ventilation, which regulate the interaction between the heart and lungs, crucial for coordinating cardiac and pulmonary processes.

Systemic arterial blood pressure (P_{as}) and systemic venous blood pressure (P_{vs}) are defined as follows:

$$\begin{cases} P_{as} = P_{dias} + \frac{1}{3}(P_{sys} - P_{dias}), \\ P_{vs} = P_{as} - F_s R_s, \end{cases}$$

these definitions are derived from [22], where P_{sys} and P_{dias} represent systolic and diastolic arterial pressures, respectively. F_s represents the blood circulation entering the tissue segment, while R_s symbolizes the resistance encountered in the systemic circuit. The value $F_s(t)$ is given by

$$F_s(t) = \frac{P_{as}(t) - P_{vs}(t)}{R_s}. (2.1)$$

This system of cardiovascular-respiratory is interconnected with the other organs and tissues of the human body. The diagram that shows the developed mathematical model is shown in the figure 1,



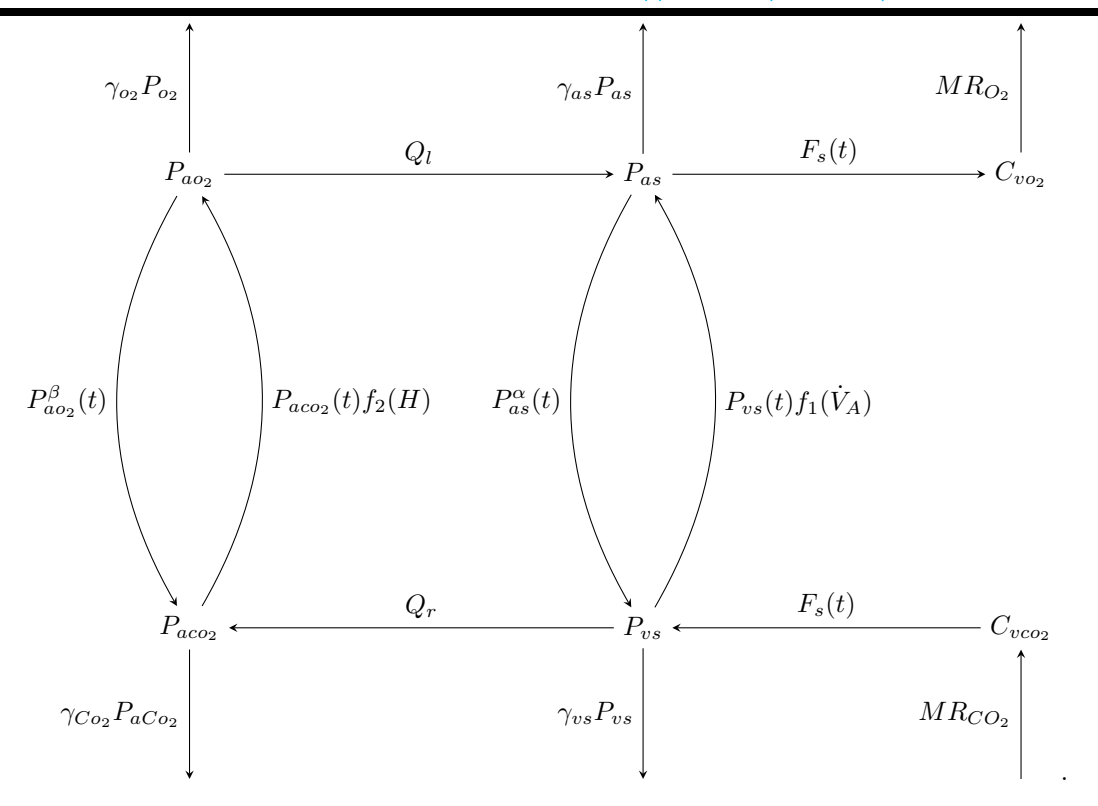


Figure 1: Diagram of mathematical model

By considering the interactions of hemodynamic measurements depicted in Figure 1, the model equations transform as stated below,

$$\begin{cases}
\frac{dP_{as}(t)}{dt} = -\gamma_{as}P_{as} + P_{vs}(t)f_{1}(\dot{V}_{A}), \\
\frac{dP_{vs}(t)}{dt} = -\gamma_{vs}P_{vs} + P_{as}^{\alpha}(t), \\
\frac{dP_{ao_{2}}(t)}{dt} = -\gamma_{o_{2}}P_{ao_{2}} + P_{aco_{2}}(t)f_{2}(H), \\
\frac{dP_{aco_{2}}(t)}{dt} = -\gamma_{co_{2}}P_{aco_{2}} + P_{ao_{2}}^{\beta}(t), \\
V_{To_{2}}\frac{dC_{vo_{2}}(t)}{dt} = -MR_{o_{2}}(t) + F_{s}(t)(C_{ao_{2}}(t) - C_{vo_{2}}(t)), \\
V_{Tco_{2}}\frac{dC_{vco_{2}}(t)}{dt} = MR_{co_{2}}(t) + F_{s}(t)(C_{aco_{2}}(t) - C_{vco_{2}}(t)),
\end{cases}$$
(2.2)

the values of the constants γ_{as} , γ_{vs} , γ_{o_2} , γ_{co_2} , α and β must be determined for the equations (2.2). It is also necessary to understand the logistic functions (2.3). The terms V_{TO_2} and V_{TCO_2} in equation (2.2) of the model stand for the tissues' efficient volume for storing oxygen and carbon dioxide, respectively, and $f_1(H), f_2(V_A)$ are represents a recognizable logistic function in the structure of the form

$$\begin{cases}
f_1(\dot{V}_A) = \frac{g_1 f_1(0)}{f_1(0) + (g_1 - f_1(0))e^{-x_1\dot{V}_A}}, \\
f_2(H) = \frac{g_2 f_2(0)}{f_2(0) + (g_2 - f_2(0))e^{-x_2 H}},
\end{cases} (2.3)$$

where x_1 and x_2 refer to the of largest growth rates of alveolar ventilation and heart rate, while g_1 and g_2 indicate the carrying capacity of alveolar ventilation and heart rate respectively. The initial

HTTPS://DOI.ORG/10.5281/ZENODO.17584815

values of $f_1(V_A)$ and $f_2(H)$ at the start of the process are represented by the constants $f_1(0)$ and $f_2(0)$ |19|.

The values $MR_{O_2}(t)$ and $MR_{CO_2}(t)$ represent the rates of metabolic oxygen consumption and metabolic carbon dioxide production, respectively, during periods of physical activity. Unfortunately, we can suggest that the rate of oxygen consumption in metabolism, denoted as $MR_{O_2}(t)$, increases in an exponential manner from the unchanging starting point $MR_{O_2}^r$ to a fresh consistent level known as $MR_{O_2}^e$ [13], the equation showing the relation is

$$MR_{O_2}(t) = MR_{O_2}^r + \left(MR_{O_2}^e - MR_{O_2}^r\right)\left(1 - e^{\frac{-t}{T_a}}\right),$$
 (2.4)

where $MR_{O_2}^r$ represents the rate of oxygen consumed by metabolic during periods of rest (inactivity) and $MR_{O_2}^e$ represents the oxygen consumption rate for metabolism during exercises (physical activity). The exponential function's time constant " T_a " can be selected as per recommendation [13], said $T_a = 0.5$ and it's configured in a way that, after every $4T_a$ minutes, the immediate oxygen supply reaches 98% of the overall oxygen requirement.

The rise in metabolic speed corresponds directly to the amount of workload undertaken. Just like the approach employed by [23], we make use of the correlation between these factors. The use of correlation between those factors is formulated as follows

$$MR_{O_2}^e = MR_{O_2}^r + \rho W,$$
 (2.5)

the parameter ρ indicates the physical state of the individual during in the exercise and W is workload. Moreover, the carbon dioxide generation rate, denoted as $MR_{CO_2}(t)$, is consistently linked to the oxygen utilization $MR_{O_2}(t)$ at each moment is given by

$$MR_{CO_2}(t) = RQMR_{O_2}(t),$$
 (2.6)

where RQ represents the unchanging respiratory quotient [13]. furthermore, there exists a connection between the arterial gas concentrations and their corresponding partial pressures as described by the dissociation laws

$$\begin{cases}
C_{ao_2}(t) = K_1 \left(1 - Ke^{-K_2 P_{ao_2}(t)} \right)^2, \\
C_{aco_2}(t) = K_{co_2} P_{aco_2}(t) + k_{co_2},
\end{cases}$$
(2.7)

the above equation are derived in [13]. The formulae used for calculating alveolar ventilation is

$$\dot{V}_A = f(VT - VD),\tag{2.8}$$

in simpler terms, "VT" stands for the denotes tidal volume, "VD" is is physiologic dead space, and "f"indicates how many breaths are taken in a minute. In numerical simulations, both f and VDare treated as constants. Respiratory physiology provides a means to determine tidal volume from the vital capacity (VC) determined in [13]

$$VC = VT + IRV + ERV, (2.9)$$

where IRV represents the inspiratory reserve volume, and ERV stands for expiratory reserve volume. These specific parameters have been sourced from existing literature. Now, we will provide the formula for estimating vital capacity, taking into account the influence of gender, height, and age on this physiological measure. The formulas to estimate vital capacity are [24]

$$VC_{male} = (27.63 - 0.0112a)h, (2.10)$$

$$VC_{female} = (21.78 - 0.0101a)h,$$
 (2.11)

where a is age in years, and h is height in cm. Table 1 shows the value parameters from the literature in [13], and the Table 2 indicate the values of IRV and ERV as found in reference [19] respectively,

The carrying capacity for the logistic function is determined based on the maximum of two factors: alveolar ventilation (V_A) and heart rate (H). Let's denote these factors as g_1 and g_2 respectively. In [19] $g_1 = 11$ and $g_2 = 115$ are considered as the carrying capacities for the logistic function, as defined in system (2.3).

Parameter	Value	Unit	Parameter	Value	Value
V_{To_2}	6	liter	V_{Tco_2}	15	liter
ρ	-0.002	-	RQ	0.88	-
$MR_{o_2}^r$	0.350	$liter_{STPD}/Min$	W	75	watt
R_s	14.8	mmHg.min/liter	$Q = F_s$	6.35	liter/Min
f	15	BPM	VD	0.15	liter
K_1	0.2	-	K_2	0.046	-
K_{co2}	0.0065	-	k_{co}	0.244	-

Table 1: Parameters from literature

	Parameter	Male	Female
ſ	IRV	3000	2100
	ERV	1100	800

Table 2: The values of IRV and ERV

Model stability analysis 2.3

Let us set $X = [P_{as}, P_{vs}, P_{ao_2}, P_{aco_2}, C_{vo_2}, C_{vco_2}]^T$ as vector state with their corresponding equilibrium state $X^e = [P_{as}^e, P_{vs}^e, P_{ao_2}^e, P_{aco_2}^e, C_{vo_2}^e, C_{vco_2}^e]^T$, and consider \dot{V}_A^e and H^e equilibrium values of alveolar ventilation and heart rate respectively. To determine the equilibrium state of a mathematical model, we need to solve the following system

$$\begin{cases}
-\gamma_{as}P_{as}^{e} + P_{vs}^{e}f_{1e} = 0, \\
-\gamma_{vs}P_{vs}^{e} + (P_{as}^{e})^{\alpha} = 0, \\
-\gamma_{o_{2}}P_{ao_{2}}^{e} + P_{aco_{2}}^{e}f_{2e} = 0, \\
-\gamma_{co_{2}}P_{aco_{2}}^{e} + (P_{ao_{2}}^{e})^{\beta} = 0, \\
-MR_{o_{2}} + \frac{P_{as}^{e} - P_{vs}^{e}}{R_{s}}(C_{ao_{2}}^{e} - C_{vo_{2}}^{e}) = 0, \\
MR_{co_{2}} + \frac{P_{as}^{e} - P_{vs}^{e}}{R_{s}}(C_{aco_{2}}^{e} - C_{vco_{2}}^{e}) = 0.
\end{cases}$$
(2.12)

Thus, after solving equation (2.12), the equilibrium point X^e of the model equation (2.2) is defined by:

$$\begin{cases} P_{as}^{e} = (\gamma_{vs}\gamma_{as})^{\frac{1}{\alpha-1}} (f_{1e})^{\frac{1}{1-\alpha}}, \\ P_{vs}^{e} = (\gamma_{vs}(\gamma_{as})^{\alpha})^{\frac{1}{\alpha-1}} (f_{1e})^{\frac{1}{1-\alpha}}, \\ P_{vo}^{e} = (\gamma_{aco_{2}}\gamma_{ao_{2}})^{\frac{1}{\beta-1}} (f_{2e})^{\frac{1}{1-\beta}}, \\ P_{aco_{2}}^{e} = (\gamma_{aco_{2}}(\gamma_{ao_{2}})^{\beta})^{\frac{1}{\beta-1}} (f_{2e})^{\frac{\beta}{1-\beta}}, \\ P_{aco_{2}}^{e} = (\gamma_{aco_{2}}(\gamma_{ao_{2}})^{\beta})^{\frac{1}{\beta-1}} (f_{2e})^{\frac{\beta}{1-\beta}}, \\ C_{vo_{2}}^{e} = C_{ao_{2}} - \frac{R_{s}MR_{o_{2}}(\gamma_{vs}\gamma_{as})^{\frac{1}{1-\alpha}} (f_{1e})^{\frac{\alpha}{\alpha-1}}}{(f_{1e}-(\gamma_{as})^{\alpha-1})}, \\ C_{vco_{2}}^{e} = C_{aco_{2}} + \frac{R_{s}MR_{co_{2}}(\gamma_{vs}\gamma_{as})^{\frac{1}{1-\alpha}} (f_{1e})^{\frac{\alpha}{\alpha-1}}}{(f_{1e}-(\gamma_{as})^{\alpha-1})}. \end{cases}$$

$$(2.13)$$

Let us compute the Jacobian matrix. By setting $G(X) = [G_1(X), G_2(X), G_3(X), G_4(X), G_5(X), G_6(X)]^T$, the model system (2.2) becomes

$$\frac{dX}{dt} = G(X),\tag{2.14}$$

where

$$\begin{cases}
G_{1}(X) = -\gamma_{as}P_{as} + P_{vs}(t)f_{1}(\dot{V}_{A}), \\
G_{2}(X) = -\gamma_{vs}P_{vs} + P_{as}^{\alpha}(t), \\
G_{3}(X) = -\gamma_{o2}P_{ao2} + P_{aco2}(t)f_{2}(H), \\
G_{4}(X) = -\gamma_{co_{2}}P_{aco_{2}} + P_{ao_{2}}^{\beta}(t), \\
G_{5}(X) = \frac{-MR_{o_{2}}(t)}{V_{To_{2}}} + \frac{P_{as}(t) - P_{vs}(t)}{R_{s}V_{To_{2}}}(C_{ao_{2}}(t) - C_{vo_{2}}(t)), \\
G_{6}(X) = \frac{MR_{co_{2}}(t)}{V_{Tco_{2}}} + \frac{P_{as}(t) - P_{vs}(t)}{R_{s}V_{Tco_{2}}}(C_{aco_{2}}(t) - C_{vco_{2}}(t)).
\end{cases}$$
(2.15)





Linearize the model system (2.2) around the equilibrium point, by taking

$$\begin{cases} \frac{C_{ao_2} - C^e_{vo_2}}{R_s V_{To_2}} = p, \\ \frac{P^e_{as} - P^e_{vs}}{R_s V_{To_2}} = y, \\ \frac{C_{aco_2} - C^e_{vco_2}}{R_s V_{Tco_2}} = z, \\ \frac{P^e_{as} - P^e_{vs}}{R_s V_{Tco_2}} = n, \end{cases}$$

Jacobian matrix $J(X^e)$ is written as follows

$$J(X^e) = \begin{pmatrix} -\gamma_{as} & f_{1e} & 0 & 0 & 0 & 0\\ \alpha(P_{as}^e)^{\alpha-1} & -\gamma_{vs} & 0 & 0 & 0 & 0\\ 0 & 0 & -\gamma_{o_2} & f_{2e} & 0 & 0\\ 0 & 0 & \beta(P_{ao_2}^e)^{\beta-1} & -\gamma_{co_2} & 0 & 0\\ p & -p & 0 & 0 & -y & 0\\ z & -z & 0 & 0 & 0 & -n \end{pmatrix}.$$

Hence, the characteristic polynomial $p(\lambda)$ is essential because it allows us to determine the eigenvalues of a Jacobian matrix. It is given by: $p(\lambda) = \det(J(X^e) - I\lambda)$, that is

$$p(\lambda) = (n+\lambda)(y+\lambda)\left((\gamma_{as} + \lambda)(\gamma_{vs} + \lambda) - \alpha(P_{as}^e)^{\alpha-1}f_{1e}\right)$$
$$\left((\gamma_{o_2} + \lambda)(\gamma_{co_2} + \lambda) - \beta(P_{ao_2}^e)^{\beta-1}f_{2e}\right).$$

Then eigenvalues becomes

$$\begin{cases} \lambda_{1} = -n, \\ \lambda_{2} = -y, \\ \lambda_{3} = \frac{-(\gamma_{as} + \gamma_{vs}) + \sqrt{\gamma_{as}^{2} + \gamma_{vs}^{2} - 2\gamma_{as}\gamma_{vs} + 4\alpha(P_{as}^{e})^{\alpha - 1}f_{1e}}}{2}, \\ \lambda_{4} = \frac{-(\gamma_{as} + \gamma_{vs}) - \sqrt{\gamma_{as}^{2} + \gamma_{vs}^{2} - 2\gamma_{as}\gamma_{vs} + 4\alpha(P_{as}^{e})^{\alpha - 1}f_{1e}}}{2}, \\ \lambda_{5} = \frac{-(\gamma_{o_{2}} + \gamma_{co_{2}}) + \sqrt{\gamma_{o_{2}}^{2} + \gamma_{co_{2}}^{2} - 2\gamma_{o_{2}}\gamma_{co_{2}} + 4\beta(P_{ao_{2}}^{e})^{\beta - 1}f_{2e}}}{2}, \\ \lambda_{6} = \frac{-(\gamma_{o_{2}} + \gamma_{co_{2}}) - \sqrt{\gamma_{o_{2}}^{2} + \gamma_{co_{2}}^{2} - 2\gamma_{o_{2}}\gamma_{co_{2}} + 4\beta(P_{ao_{2}}^{e})^{\beta - 1}f_{2e}}}{2}. \end{cases}$$

Theorem 2.1. If all eigenvalues are negative, the system is stable, conversely, if any eigenvalue is a positive, the system is unstable. This is proved in [20]

The equilibrium point is is asymptotically stable when all eigenenvalues are strictly negative, this condition is obeyed when $P^e_{vs} < P^e_{as}, \ P^e_{as} < \frac{(\gamma_{vs}\gamma_{as})^{\frac{1}{\alpha-1}} \left(f_1(\dot{V}_A)\right)^{\frac{1}{1-\alpha}}}{\alpha^{\frac{1}{\alpha-1}}}, \ \text{and} \ P^e_{ao_2} < \frac{\left(\gamma_{aco_2}\gamma_{ao_2}\right)^{\frac{1}{\beta-1}} \left(f_2(H)\right)^{\frac{1}{1-\beta}}}{\beta^{\frac{1}{\beta-1}}}.$ Otherwise it is unstable.

It can be readily shown that the function G is differentiable with respect to X. As a result, it is locally Lipschitz continuous in the variable X. Moreover, by applying the Cauchy-Lipschitz theorem [21], we arrive at the following result.

Theorem 2.2. Given the initial condition $X_0 = \left(P_{as}^0, P_{vs}^0, P_{aO_2}^0, P_{aCO_2}^0, C_{vO_2}^0, C_{vCO_2}^0\right)^T$, there exists a time $t_1 \geq 0$ such that a unique maximal solution $X : [0, t_1] \to \mathbb{R}^6$ of class C^1 exists for equation (2.2), satisfying the initial condition $X(0) = X_0$.

The model presented here yields a maximal solution, which is not necessarily global. One particularly interesting aspect is that, in non-pathological cases, the system naturally progresses toward a stable state through an autoregulatory mechanism, here initial of the model are data measured from patient in [14].

3 Formulation of optimal control for testing homeostasis of

If $X = (P_{as}, P_{vs}, P_{aO_2}, P_{aCO_2}, C_{vO_2}, C_{vCO_2})^T$ is a state vector, then the homeostasis state is reachable due to controls of cardiovascular-respiratory system that is heart rate H and alveolar ventilation V_A . Let us

consider that the parameters H and \dot{V}_A reach their equilibrium values respectively H^e and \dot{V}_A^e , the optimal control problem can be formulated from [15], as follows.

Find H^* , \dot{V}_A^* solution of

$$\min_{H,\dot{V}_A} J(H,\dot{V}_A) = \int_0^{T_{\text{max}}} \left[a_1 (P_{as}(t) - P_{as}^e)^2 + a_2 (P_{vs}(t) - P_{vs}^e)^2 + b_1 (H(t) - H^e)^2 + b_2 \left(\dot{V}_A(t) - \dot{V}_A^e\right)^2 \right] dt$$
(3.1)

subject to equation (2.2).

The positive scalar coefficients a_1 , a_2 , b_1 and b_2 determine how much weight is attached to each cost component term in the integrand whereas T_{max} denotes the maximum time that the control can be done.

To find the discrete form of the mathematical model (2.2), we take a linear B-splines basis functions

$$\mathcal{B}^{N} = \left\{ \psi_{j}^{N}, \ j = 1, ..., N \right\}, \tag{3.2}$$

on uniform grid

$$\Omega_N = \left\{ t_k = \frac{kT_{\text{max}}}{N}, \quad k = 0, ..., N \right\}$$
(3.3)

satisfying the following property

$$\psi_i^N(t_k) = \delta_{ik},$$

 $\psi_i^{:\cdot}(t_k) = \delta_{ik},$ where δ_{ik} is Kronecker symbol. Let also introduce a vector space W^N whose the basis is \mathcal{B}^N . It verifies

- $\dim W^N = N$,
- \bullet $W^N \subset W^{N+1}$

Taking $W = C^{0}(0,T)$ and interpolation operator

$$\Pi^{N} : W \longrightarrow W^{N}
\phi \longmapsto \Pi^{N} \phi,$$
(3.4)

satisfying

$$\Pi^{N} \phi(t_k) = \phi(t_k), \quad k = 1, \dots, N.$$
(3.5)

Then we have

$$\left\| \Pi^N \phi - \phi \right\|_{E} \xrightarrow{N \to \infty} 0 \quad \forall \phi \in W,$$
 (3.6)

$$\left|\left|\left|\Pi^{N}\right|\right|\right| = \sup_{\substack{\phi \neq W \\ \phi \neq W}} \frac{\left\|\Pi^{N}\phi\right\|_{W}}{\left\|\phi\right\|_{W}} = 1.$$

$$(3.7)$$

Now, let us set

$$f_1^N = \Pi^N f_1 = \sum_{k=0}^N f_1^k \psi_k^N \text{ and } f_2^N = \Pi^N f_2 = \sum_{k=0}^N f_2^k \psi_k^N,$$

where

$$f_1^k = f_1(\dot{V}_A(t_k)), \quad f_2^k = f_2(H(t_k)).$$

Hence, the system (2.2) can be approached by the following problem. Find $(x^N, y^N, v^N) \in (W^N)^3$ solution of the system

$$\begin{cases}
\frac{dP_{as}^{N}(t)}{dt} = -\gamma_{as}P_{as}^{N}(t) + P_{vs}^{N}(t)f_{1}^{N}, \\
\frac{dP_{vs}^{N}(t)}{dt} = -\gamma_{vs}P_{vs}^{N}(t) + (P_{as}^{\alpha}(t))^{N}, \\
\frac{dP_{aO_{2}}^{N}(t)}{dt} = -\gamma_{O_{2}}P_{aO_{2}}^{N}(t) + P_{aCO_{2}}^{N}(t)f_{2}^{N}, \\
\frac{dP_{aCO_{2}}^{N}(t)}{dt} = -\gamma_{CO_{2}}P_{aCO_{2}}^{N}(t) + (P_{aO_{2}}^{\beta}(t))^{N}, \\
V_{TO_{2}}\frac{dC_{vO_{2}}^{N}(t)}{dt} = -MR_{O_{2}}(t) + \frac{P_{as}^{N}(t) - P_{vs}^{N}(t)}{R_{s}} \left(C_{aO_{2}}^{N}(t) - C_{vO_{2}}^{N}(t)\right), \\
V_{TCO_{2}}\frac{dC_{vCO_{2}}^{N}(t)}{dt} = MR_{CO_{2}}(t) + \frac{P_{as}^{N}(t) - P_{vs}^{N}(t)}{R_{s}} \left(C_{aCO_{2}}^{N}(t) - C_{vCO_{2}}^{N}(t)\right)
\end{cases}$$
(3.8)

11(3), 2025, Pages 49 - 67

HTTPS://DOI.ORG/10.5281/ZENODO.17584815

with

IJMSO

$$P_{as}^{N}(0) = P_{as}^{N,0}, \quad P_{vs}^{N}(0) = P_{vs}^{N,0}, \quad P_{aO_{2}}^{N}(0) = P_{aO_{3}}^{N,0},$$
 (3.9)

$$P_{aCO_2}^N(0) = P_{aCO_2}^{N,0}, \quad C_{vO_2}^N(0) = C_{vO_3}^{N,0}, \quad C_{vCO_2}^N(0) = C_{vCO_2}^{N,0},$$
 (3.10)

such that

$$\left| P_{as}^0 - P_{as}^{N,0} \right| \underset{N \to \infty}{\longrightarrow} 0, \quad \left| P_{vs}^0 - P_{vs}^{N,0} \right| \underset{N \to \infty}{\longrightarrow} 0,$$
 (3.11)

$$\left| P_{aO_2}^0 - P_{aO_2}^{N,0} \right| \underset{N \to \infty}{\longrightarrow} 0, \quad \left| P_{aCO_2}^0 - P_{aCO_2}^{N,0} \right| \underset{N \to \infty}{\longrightarrow} 0, \tag{3.12}$$

$$\left| C_{vO_2}^0 - C_{vO_2}^{N,0} \right| \underset{N \to \infty}{\longrightarrow} 0 \underset{N \to \infty}{\longrightarrow} 0, \quad \left| C_{vCO_2}^0 - C_{vCO_2}^{N,0} \right| \underset{N \to \infty}{\longrightarrow} 0.$$
 (3.13)

We have the following result with the proof provided in [25].

Proposition 3.1. The solution sequence of the system (3.8) converges uniformly toward the solution of the system (2.2) on the interval $[0, T_{\text{max}}], T_{\text{max}} > 0$.

To approximate the optimal problem (3.1)-(2.2), let us set $x=(P_{as},P_{vs})^T$ the state vector, $x^0=(P_{as}^0,P_{vs}^0)^T$ the initial state vector, $x^e=(P_{as}^e,P_{vs}^e)^T$ the wanted equilibrium state vector, $\lambda=(H,V_A)^T$ the control vector and $\lambda^e = (H^e, \dot{V}_A^e)^T$ the equilibrium control vector; $x_i, x_i^0, x_i^e, \lambda_i$ and λ_i^e denote the ith components ith of the vector x, x^0 , x^e , λ and λ^e .

Therefore, the problem (3.1)-(2.2) can take the following compact form

$$\min_{\lambda \in Q} J^{N}(\lambda) = \int_{0}^{T_{\text{max}}} \left(\sum_{i=1}^{2} a_{i} (x_{i}^{N}(t) - x_{i}^{e})^{2} + \sum_{j=1}^{2} b_{j} (\lambda_{j} - \lambda_{j}^{e})^{2} \right) dt$$
(3.14)

where $x^N = (x_1^N, x_2^N)^T$ is the approximated solution of $(P_{as}, P_{vs})^T$ obtained from (3.8). We must determine $\lambda^M = (\lambda_1^M, \lambda_2^M) \in Q^M$ an approximate solution of (3.14) in $Q^M = (W^M)^2$. Note that we can write

$$\lambda_j^M = \sum_{k=0}^M \lambda_{j,k}^M \psi_k(t), \ j = 1, 2.$$

Therefore, we can approximate the cost function (3.14) as follows

$$\min_{\lambda \in Q} J^{N}(\lambda) = \sum_{k=1}^{M} \left(\sum_{i=1}^{2} a_{i} (x_{i}^{N}(t_{k}) - x_{i}^{e})^{2} + \sum_{j=1}^{2} b_{j} (\lambda_{j,k}^{M} - \lambda_{j}^{e})^{2} \right) \Delta t, \tag{3.15}$$

where $\Delta t = \frac{T_{\text{max}}}{N}$. The convergence of the discreet objective function (3.15) toward the continous objective function given by the problem (3.14) has been proven in [25]. Finally, the optimal control problem (3.1)-(2.2) is a minimisation problem with constraint. The discreet formulation of such problem can be written

Find $\lambda^{*,M} \in \mathbb{R}^{(M+1)} \times \mathbb{R}^{(M+1)}$ solution of

$$\min_{\lambda^M \in \mathbb{R}^{(M+1)} \times \mathbb{R}^{(M+1)}} J^N(\underline{\lambda}^M) \approx \Delta t \left((Y^T A Y) + \left(\underline{\lambda}^M \right)^T B \underline{\lambda}^M \right), \tag{3.16}$$

subject to (3.8) where

$$A = \left(\begin{array}{cc} a_1 & 0 \\ 0 & a_2 \end{array}\right), \qquad B = \left(\begin{array}{cc} b_1 & 0 \\ 0 & b_2 \end{array}\right).$$

subject to (3.8), where λ^M is a matrix $(M+1)\times 2$ such that the components $\lambda^M_{j,k}$ are those function λ^N_j in \mathcal{B}^N and Y is the matrix such that the $(i,k)^{th}$ component is $(x^N_i(t_k)-x^e_i)$ with where $x^N=(x^N_1,x^N_2)^T$ is the solution of (3.1)-(2.2) associated to $\lambda = \lambda^N$.

The equilibrium value of alveolar ventilation is determined by the vital capacity provided by equations (2.10) and (2.11). For males aged a = 50 years and height h = 170 cm, equation (2.10) yields

$$VC_{\text{male}} = (27.63 - 0.0112 \times 50) \times 170 = 4601.9 \,\text{ml}.$$
 (3.17)

Using equations (2.9) and (3.17), and the values from Table 2, the tidal volume for males is

$$VT_{\text{male}} = VC_{\text{male}} - (IRV_{\text{male}} + ERV_{\text{male}}) = 501.9 \,\text{ml}. \tag{3.18}$$

11(3), 2025, Pages 49 - 67

HTTPS://DOI.ORG/10.5281/ZENODO.17584815

Thus, according to equations (2.8) and (3.18), and the values in Table 1, the equilibrium value of alveolar ventilation for males is

$$\dot{V}_{A_{\text{male}}}^e = f(VT - VD) = 15(0.5019 - 0.15) \text{ liters/min} = 5.3 \text{ liters/min}.$$
 (3.19)

Similarly, for females with a = 45 years and h = 165 cm, equation (2.11) yields

IJMSO

$$VC_{\text{female}} = (21.78 - 0.101 \times 45) \times 165 = 3518.7 \,\text{ml}.$$
 (3.20)

Using equations (2.9) and (3.20), and the reference to Table 2, the tidal volume for females is

$$VT_{\text{female}} = VC_{\text{female}} - (IRV_{\text{female}} + ERV_{\text{female}}) = 618.7 \,\text{ml}.$$
 (3.21)

Thus, according to equations (2.8) and (3.21), and the values in Table 1, the equilibrium value of alveolar ventilation for females is

$$\dot{V}^e_{A_{\rm female}} = f(VT - VD) = 15(0.6187 - 0.15) \, \text{liters/min} = 7.0 \, \text{liters/min}. \tag{3.22}$$

In a healthy state, an individual's heart rate typically stabilizes within the normal range. According to Ho (2014), a normal adult heart rate generally falls between 60 to 100 beats per minute [26]. For our considerations, we assume $H_{\text{female}}^e = 100 \text{ beats/min and } H_{\text{male}}^e = 85 \text{ beats/min.}$

The model parameters are computed by fitting the mathematical model to simulation results obtained from Timischl's model. The MATLAB's built-in function fmincon is very important and is used to minimize cost function subject to a given constraint [27]. Now it can be used to solve (3.16) subject discretized equation (3.8). The parameters are then detailed in Table 3.

Parameter	male	female	Parameter	male	female
α	0.0632	0.0831	γ_{as}	0.4217	0.4342
β	0.4301	0.4601	γ_{vs}	0.2903	0.2873
γ_{o_2}	27.9872	30.5214	x_1	1.0007	1.2147
x_2	0.1081	0.2018	γ_{co_2}	0.2845	0.2825

Table 3: Estimated parameters

Using the estimated values in The table 3 and system (2.13) we have the following equilibrium values for each model variables in the Table 4.

Variable	Female	Male	Variable	Female	Male
P_{as}^{e}	118.6242	115.5674	$P^e_{aco_2}$	28.4217	25.9273
P_{vs}^e	4.6824	4.6508	$C_{vo_2}^e$	0.1644	0.1602
$P_{ao_2}^e$	108.9002	105.3088	$C^e_{vco_2}$	0.4973	0.4912

Table 4: Equilibrium values

Implementation of the designed Matlab GUI 4

The implementation of the designed Matlab GUI was accomplished using the App Designer tool. This powerful feature in Matlab allows for the creation of professional apps with user-friendly interfaces. By leveraging the App Designer, we were able to incorporate interactive elements, streamline user inputs, and enhance overall functionality. The resulting GUI provides an efficient and intuitive platform for users to interact with the underlying mathematical model and simulations.

We are going to present the Matlab GUI design of the developed model, detailing the interface's layout and functionality. This GUI facilitates user interaction and enhances the overall usability of the model.

4.1 Matlab GUI design of the developed model

To design this GUI using developed mathematical model of cardiovascular-respiratory system. A GUI (Graphical User Interface) created in MATLAB App Designer is an interface generated through the App Designer tool, enabling developers to create interactive and user-friendly applications. The GUI has been

OPTIMIZATION: THEORY AND APPLICATIONS 11(3), 2025, Pages 49 - 67

HTTPS://DOI.ORG/10.5281/ZENODO.17584815

created in MATLAB App Designer using the developed mathematical model of the human body. It is taken into account when we regard the following parameters as input in the GUI. These input parameters include age (a), height (h), heart rate (H), systolic arterial pressure (P_{sys}) , diastolic arterial pressure (P_{dias}) , arterial oxygen pressure (P_{aO_2}) , arterial carbon dioxide pressure (P_{aCO_2}) , venous oxygen concentration (C_{vO_2}) , and venous carbon dioxide concentration (C_{vCO_2}) .

The design typically includes elements or components, each assigned to correspond to specific variables or functions within the MATLAB code. To run the GUI and obtain outputs, one typically initiates the MATLAB script containing the GUI code, which generates the interface. Users then interact with the GUI by adjusting inputting values, or clicking buttons as designed, which triggers the underlying functions and updates the displayed outputs or plots accordingly. Running the GUI code thus activates the following GUI defined in figure 2, allowing users to manipulate parameters and visualize results within the interface.

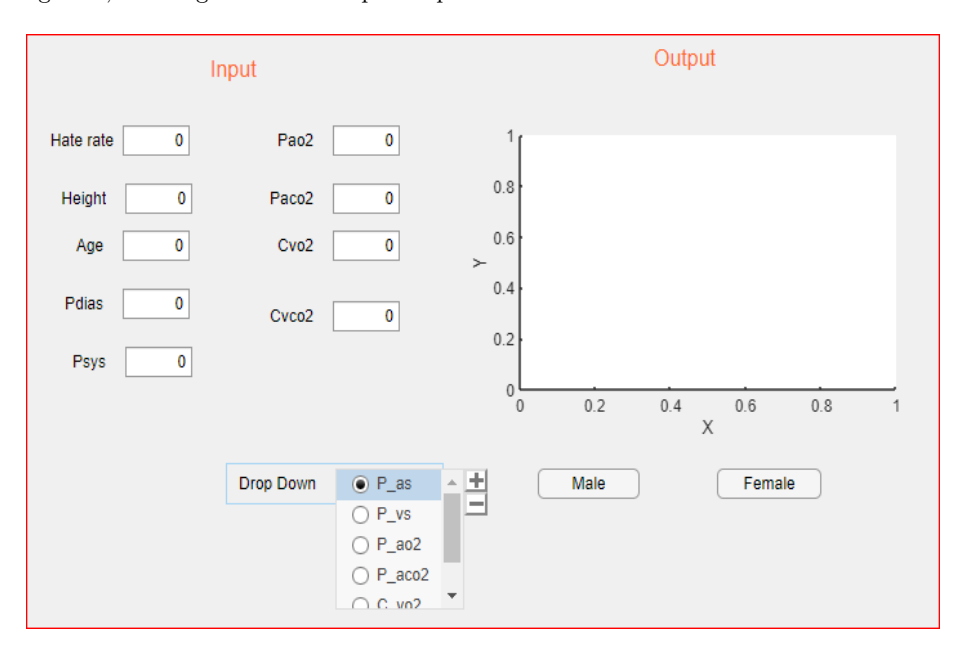


Figure 2: Designed GUI

Once this GUI is displayed, interact with the provided input fields or buttons as specified. Input required data or parameters into the designated areas or select the desired options within the GUI interface. After providing the necessary inputs, select the desired option from the Dropdown component, and trigger the processing or calculation by clicking the designated female or male button. This function processes the selected input and generates the output or result associated with that particular choice. The GUI will then execute the underlying code, perform the specified operations, and display the outputs within the GUI interface itself. Review these output areas to observe the results generated by the executed code through

We delves into the practical steps involved in bringing the designed graphical user interface (GUI) to life. It outlines the implementation process, detailing the tools, technologies, and methodologies employed to transform the conceptual design into a functional and user-friendly interface.

Implementation of the designed GUI 4.2

In this paper, we require the outcomes of a global mathematical model of the cardiovascular respiratory system developed in [13]. Upon solving Timischl's mathematical model using a built-in MATLAB ODE solver both healthy and unhealthy condition, the results are presented in a custom-designed GUI output to assess the fidelity of the GUI. After computing all model parameters we use the data collected in [14] for testing the behaviors of our GUI and we have chosen female button because the data refer to female.





In situations where the input corresponds to the healthy subject, as shown in Figure 2, the resulting output are depicted in Figures 3, 4, and 5.

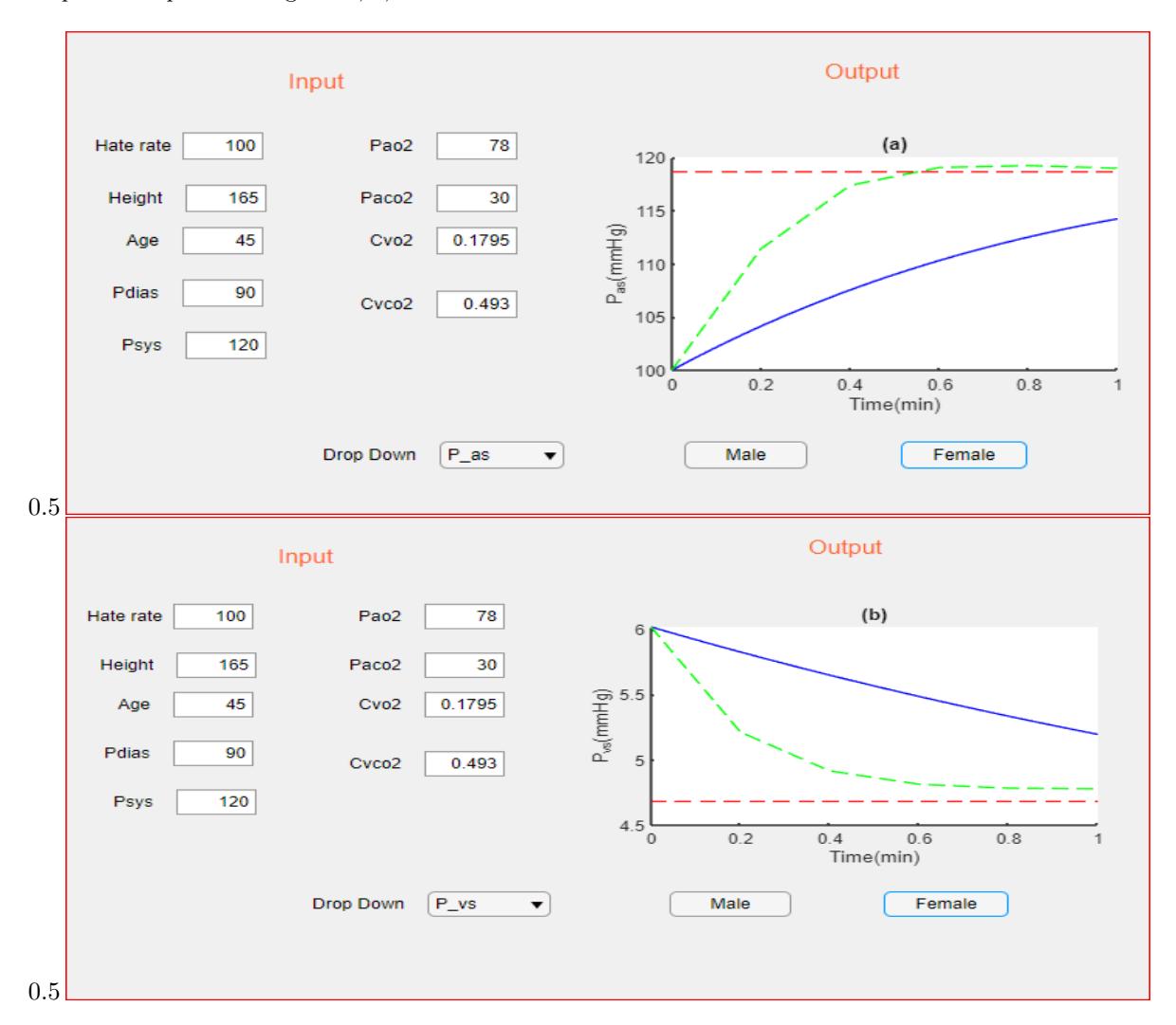


Figure 3: Output trends of systemic arterial pressure (a) and systemic venous pressure (b) using input of healthy subject in designed GUI solid line compared to one from the computation of Timischl's model (dashed green line)and equilibrium value (dashed red line)

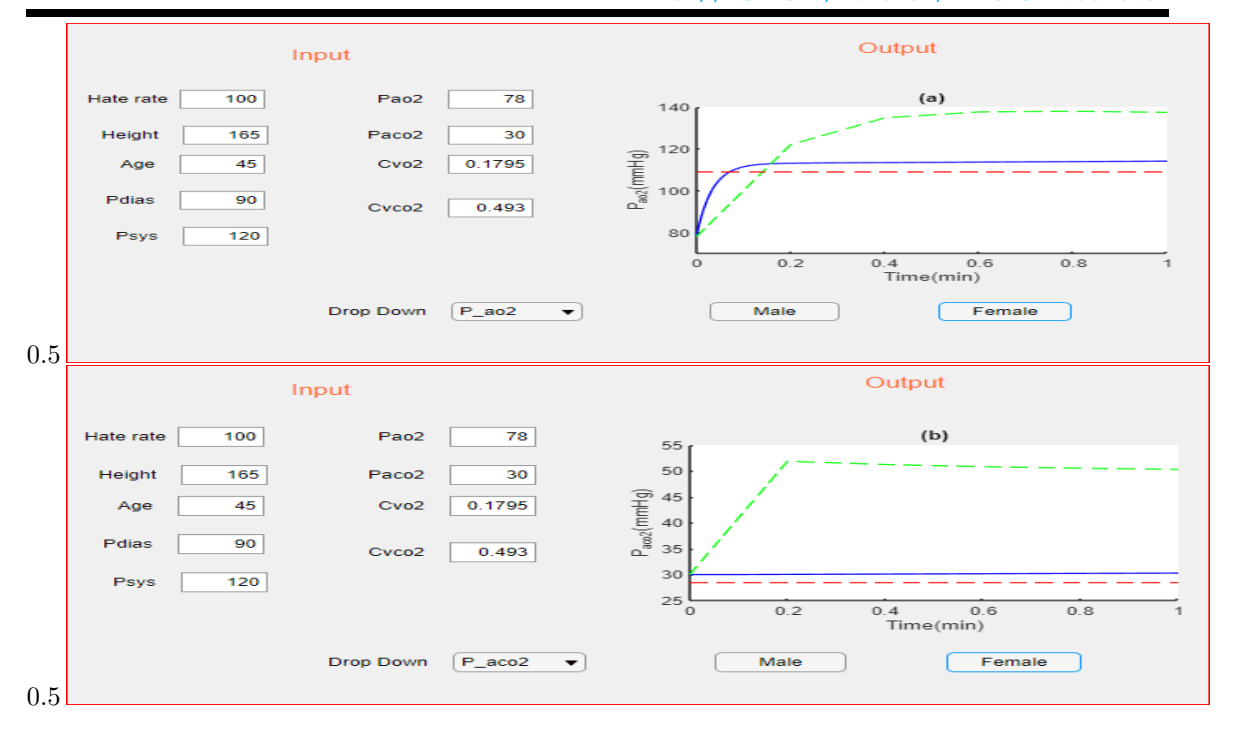


Figure 4: Output trends of arterial oxygen partial pressure (a) and arterial carbon dioxide partial pressure (b) using input of healthy subject in designed GUI solid line compared to one from the computation of Timischl's model (dashed line) and equilibrium value (dashed red line)

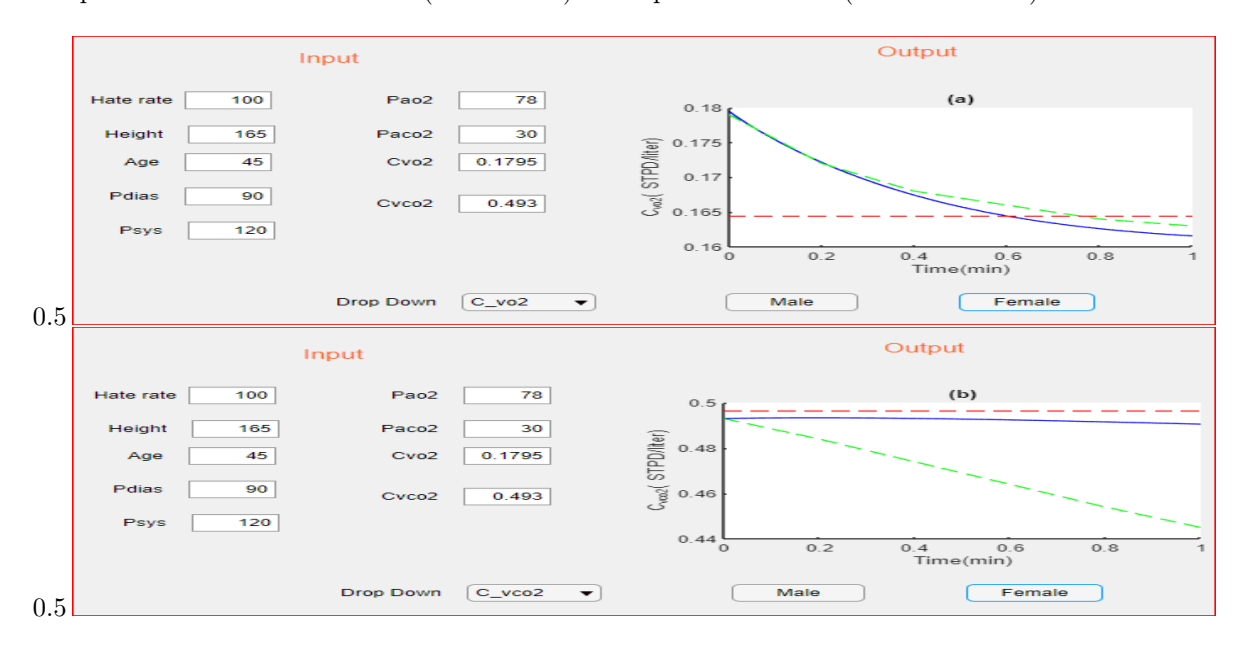


Figure 5: Output trends of concentration of oxygen in venous (a) and concentration of carbon dioxide in venous (b) using the input of healthy subject in designed GUI solid line compared to one from the computation of Timischl's model (dashed line) and equilibrium value (dashed red line)

11(3), 2025, PAGES 49 - 67

HTTPS://DOI.ORG/10.5281/ZENODO.17584815

Now, our attention shifts to the homeostasis of the model variables. In this context, we examine the model solutions depicted in Figures 3, 4, and 5. Homeostasis is confirmed through the calculation of the mean +for each model variable. The mean values of the model variables are determined using the following relationship

$$\bar{x} = \frac{\sum_{i=0}^{n} x_i}{n+1},\tag{4.1}$$

where $x_i = x(t_i)$ and i = 0, 1, 2, ..., n, with n total of the taken sub intervals, the mean are presented in the table 5.

Variable	Values	Variable	Values
P_{as}	112.1152	P_{aco_2}	29.5662
P_{vs}	5.5862	C_{vo_2}	0.1482
P_{ao_2}	102.3900	C_{vo_2}	0.4902

Table 5: Mean of each variable from the model

The calculation of the mean values of the model variables, as depicted in Table 5, is substantiated by comparing them to the respective reference values of healthy subjects outlined in Table 6, collected in [28], [29], [30]. The graphical user interface (GUI) inputs from healthy subjects are used to create visual

	Variable	Minimum	Maximum	Variable	Minimum	Maximum
Ī	P_{as}	100	120	P_{aco_2}	35	45
	P_{vs}	5	8	C_{vo_2}	0.140	0.155
	P_{ao_2}	75	105	C_{vco_2}	0.50	0.75

Table 6: Normal range of each physiological parameter

representations for evaluating the stability of the cardiovascular and respiratory systems. These graphics aid in studying the body's regulatory mechanisms and help understand the complex balance within these systems. By leveraging GUI technology, researchers gain insights into the dynamic interactions governing cardiovascular and respiratory homeostasis. This visual approach improves our ability to assess and comprehend physiological processes, emphasizing the significance of graphical representation in advancing our understanding of health-related mechanisms.

In the case where the input, as shown in Figure 2, pertains to an unhealthy subject, it yields the corresponding outputs depicted in Figures 6, 7, and 8.

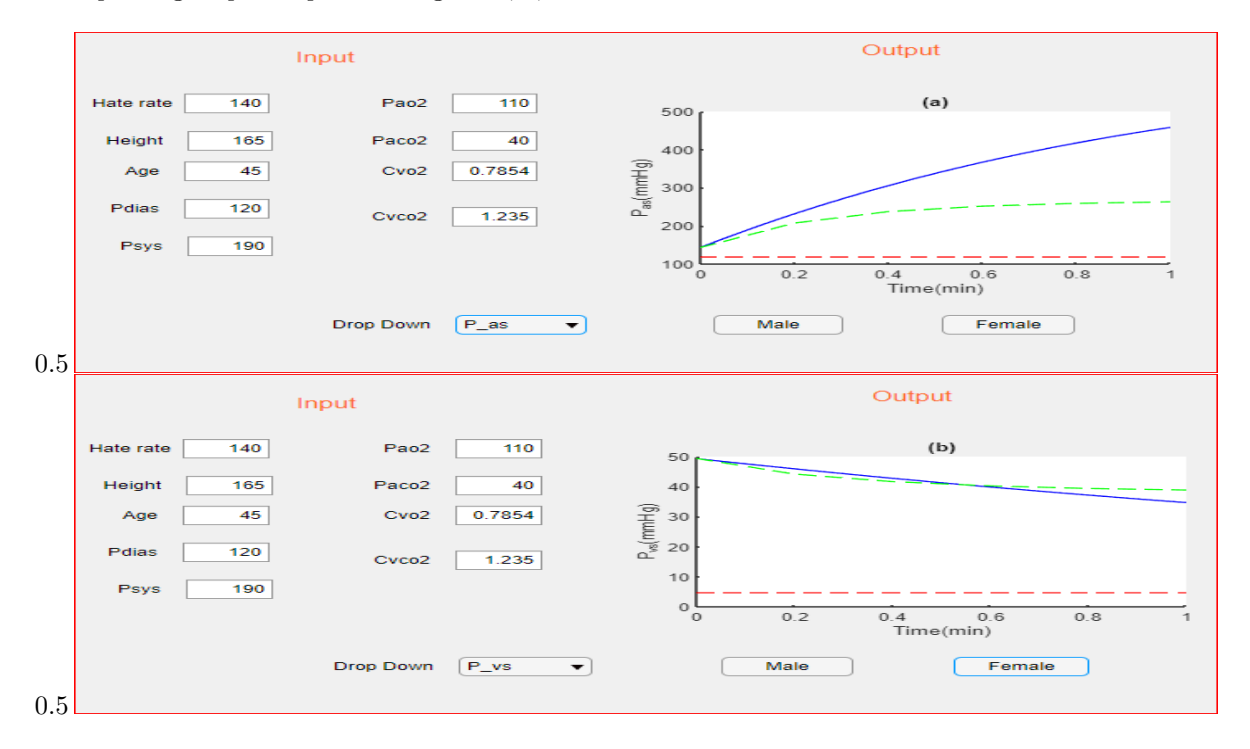


Figure 6: Output trends of systemic arterial pressure (a) and systemic venous pressure (b) using the input of abnormal subject in designed GUI solid line compared to one from the computation of Timischl's model (dashed line) and equilibrium value (dashed red line)

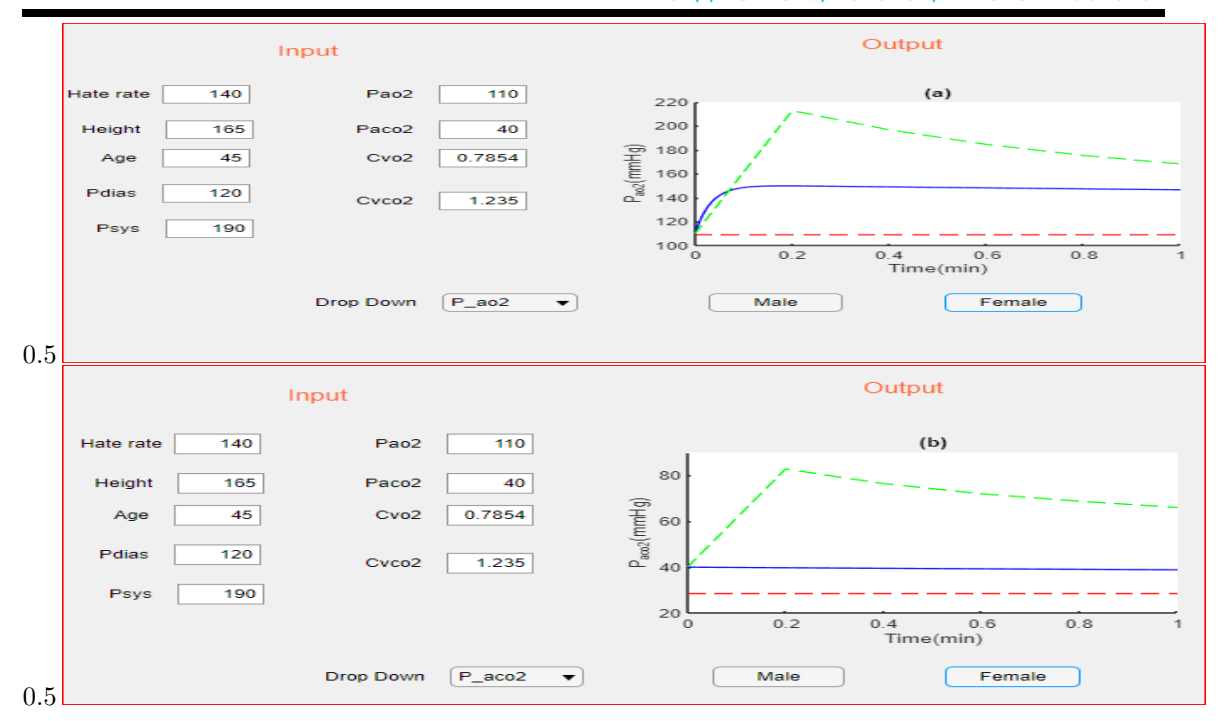


Figure 7: Output trends of arterial oxygen partial pressure (a) and arterial carbon dioxide partial pressure (b) using an input of abnormal subject in designed GUI solid line compared to one from the computation of Timischl's model (dashed line) and equilibrium value (dashed red line)

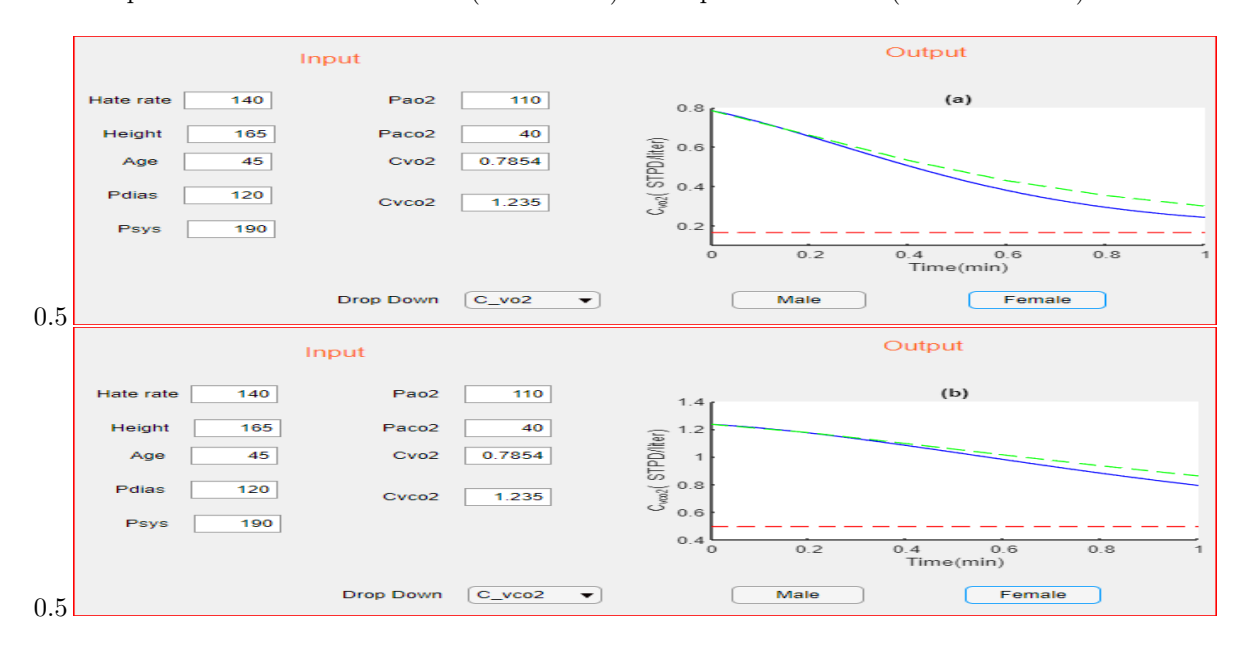


Figure 8: Output trends of concentration of oxygen in venous (a) and concentration of carbon dioxide in venous (b) using an input of abnormal subject in designed GUI solid line compared to one from the computation of Timischl's model (dashed line) and equilibrium value (dashed red line)

The Graphical User Interface (GUI) output exceeds predefined references without control measures. This highlights the need for effective controls to maintain output within acceptable bounds. Failure risks



HTTPS://DOI.ORG/10.5281/ZENODO.17584815

deviations from standards and undesirable outcomes. It's crucial to address and rectify any GUI output surpassing specified references to mitigate risks and uphold quality standards.

5 Discussion

The paper examines homeostasis in the context of cardiovascular and respiratory systems, emphasizing its crucial role in maintaining physiological equilibrium. Table 5 demonstrates that homeostasis is wellregulated, with cardiovascular and respiratory parameters consistently within normal ranges, reflecting efficient physiological function and stability despite potential fluctuations. This balance ensures optimal oxygen delivery, carbon dioxide removal, and overall circulatory efficiency, underscoring the importance of homeostasis for health. Figures 3, 4, and 5 show that the system's behavior approaches equilibrium over time, indicating effective control and stability, essential for maintaining cardiovascular and respiratory health. Conversely, Figures 6, 7, and 8 reveal instability and deviations from equilibrium in unhealthy conditions, suggesting potential dysregulation and the need for timely interventions. These deviations highlight the need for monitoring and intervention to address health issues. Additionally, a comparative analysis of the graphical user interface (GUI) with Timischl's model shows that the GUI accurately reflects the system's behavior, with close alignment between the outputs of the mathematical model and real-world observations. This validation confirms that the GUI effectively handles both healthy and unhealthy data, demonstrating its reliability in representing physiological states and maintaining health.

6 Conclusion

This study delved into the stability analysis of a mathematical model of the cardiovascular-respiratory system, employing a graphical user interface (GUI) to evaluate homeostasis in healthy individuals. The model's optimal control leveraged bodily stability to uphold homeostasis, ensuring efficient regulation of physiological functions and adaptability to internal and external changes. By integrating stability and homeostasis mechanisms within the model's control framework, it facilitated a robust response to physiological challenges, promoting overall health. The obtained results align with empirical data by showing that the GUI's outputs accurately reflect both healthy and unhealthy states as evidenced by the close correlation between the GUI's mathematical model and Timischl's real-world model. This concordance underscores the GUI's reliability in simulating physiological conditions, demonstrating that the system's behavior under various conditions matches observed data. Investigation of equilibrium points within the model revealed stability in healthy conditions and instability in unhealthy ones. The GUI's ability to display accurate representations of equilibrium in healthy states and deviations in unhealthy states makes it a valuable tool for monitoring cardiovascular and respiratory health. By visually representing these conditions, the GUI aids in diagnosing and managing health issues, making it a practical asset for both clinical and research applications. However, the GUI's limitation lies in its dependence on machine-specific software, requiring integration into MATLAB's web design for broader accessibility, which demands specialized expertise. Nevertheless, the study underscores the GUI's efficacy in assessing diseases affecting cardiovascular and respiratory systems, highlighting its potential as a valuable tool in medical research and diagnosis.

Acknowledgment

The authors sincerely appreciate and express their deep gratitude to The World Academy of Science (TWAS) for their financial support of this research through TWAS Research Grant No. 19-220 RG/MATHS/AF/AC-G - FR3240310125.

References

- [1] Cannon, W. B. (1929). Organization for physiological homeostasis. *Physiological reviews*, 9(3), 399-431.
- [2] Spyer, K. M. (1995). Central nervous mechanisms responsible for cardio-respiratory homeostasis. Control of the Cardiovascular and Respiratory Systems in Health and Disease, 73-79.
- [3] Travers, G., Kippelen, P., Trangmar, S. J., González-Alonso, J. (2022). Physiological function during exercise and environmental stress in humans—An integrative view of body systems and homeostasis. Cells, 11(3), 383.

HTTPS://DOI.ORG/10.5281/ZENODO.17584815

- [4] Ntaganda, J. M., and Mampassi, B. (2012). CARDIOGUI: An Interface Guide to Simulate Cardiovascular Respiratory System during Physical Activity, Applied Mathematics, vol. 3, no. 12.
- [5] Tu, J., Yeoh, G. H., Liu, C., Tao, Y. (2023). Computational fluid dynamics: a practical approach, Elsevier.
- [6] Müller-Putz, G. R., Breitwieser, C., Cincotti, F., Leeb, R., Schreuder, M., Leotta, F., Millán, J. D. R. (2011). Tools for brain-computer interaction: a general concept for a hybrid BCI. Frontiers in neuroinformatics, 5, 13415.
- [7] Priyam, A., Woodcroft, B. J., Rai, V., Moghul, I., Munagala, A., Ter, F., and Wurm, Y. (2019). Sequenceserver: a modern graphical user interface for custom BLAST databases. Molecular biology and evolution, 36(12), 2922-2924.
- [8] Sadeghi Milani, A., Cecil-Xavier, A., Gupta, A., Cecil, J., and Kennison, S. (2024). A systematic review of human-computer interaction (HCI) research in medical and other engineering fields. International Journal of Human-Computer Interaction, 40(3), 515-536.
- [9] Heldt, T., Mukkamala, R., Moody, G. B., and Mark, R. G. (2010).CVSim: an open-source cardiovascular simulator for teaching and research. The open pacing, electrophysiology and therapy journal, 3,
- [10] Maestri, R., and Pinna, G. D. (1998). POLYAN: a computer program for polyparametric analysis of cardio-respiratory variability signals. Computer methods and programs in biomedicine, 56(1), 37-48.
- [11] Trenhago, P. R., Fernandes, L. G., Müller, L. O., Blanco, P. J., and Feijóo, R. A. (2016). An integrated mathematical model of the cardiovascular and respiratory systems International journal for numerical methods in biomedical engineering, 32(1), e02736.
- [12] Cheng, L., Albanese, A., Ursino, M., and Chbat, N. W. (2016). An integrated mathematical model of the human cardiopulmonary system: model validation under hypercapnia and hypoxia. American Journal of Physiology-Heart and Circulatory Physiology, 310(7), H922-H937.
- [13] Timischl, S. (1998). A Global Model for the Cardiovascular and Respiratory System: diss. of the requirements for the degree Doktor Rerum Naturalium/Susanne Timischl. Karl-Franzens University of Graz.
- [14] Bizimungu, T., Harelimana, D., Marie Ntaganda, J. (2021). Client-Server and Web-Based Graphical User Interface Design for the Mathematical Model of Cardiovascular-Respiratory System. Applied Computational Intelligence and Soft Computing, 2021(1), 5581937.
- [15] Afolabi, A. S., Oyewale, A. A. (2025). On the Solutions of Optimal Control Problems Constrained by Ordinary Differential Equations with Vector-Matrix Coefficients Using FICO Xpress Mosel. International Journal of Mathematical Sciences and Optimization: Theory and Applications, 11(2), 111-132.
- [16] Grosselin, F., Navarro-Sune, X., Raux, M., Similowski, T., and Chavez, M. (2018). CARE-rCortex: A Matlab toolbox for the analysis of CArdio-REspiratory-related activity in the Cortex. Journal of Neuroscience Methods, 308, 309-316.
- [17] Schulz, S. M., Ayala, E., Dahme, B., and Ritz, T. (2009). A MATLAB toolbox for correcting withinindividual effects of respiration rate and tidal volume on respiratory sinus arrhythmia during variable breathing. Behavior Research Methods, 41, 1121-1126.
- [18] Schroeder, M. J., Perreault, B., Ewert, D. L., and Koenig, S. C. (2004). HEART: an automated beat-to-beat cardiovascular analysis package using Matlab. Computers in Biology and Medicine, 34(5), 371-388.
- [19] Ntaganda, J. M., Niyobuhungiro, J., Banzi, W., Mpinganzima, L., Minani, F., Gahutu, J. B., . Kambutse, I. (2019). Mathematical modelling of human cardiovascular-respiratory system responses to exercise in Rwanda. International Journal of Mathematical Modelling and Numerical Optimisation, 9(3), 287-308.
- [20] Perko, L. Differential equations and dynamical systems. Springer Science and Business Media, 2013.
- [21] Lelong-Ferrand, J. (1977). JM Arnaudi es. Cours de math ematiques, Tome4, Equations differentielles, int egrales multiples, Dunod Universit e, Bordas, Paris.
- [22] Klabunde, R. (2011). Cardiovascular physiology concepts. Lippincott Williams and Wilkins.
- [23] Kappel, F., Peer, R. O. (1995). Implementation of a cardiovascular model and algorithms for parameteridentification. Karl-Franzens-Univ. Graz and Techn. Univ. Graz.



HTTPS://DOI.ORG/10.5281/ZENODO.17584815

- [24] Abramowitz, S., Leiner, G. C., Lewis, W. A., Small, M. J. (1965). Vital capacity in the Negro. American Review of Respiratory Disease, 92(2), 287-292.
- [25] Ntaganda, J. M., Mampassi, B., Seck, D. (2007). Modelling blood partial pressures of the human cardiovascular/respiratory system. Applied Mathematics and computation, 187(2), 1100-1108.
- [26] Ho, K. K. L. (2014). The long-term prognostic value of heart rate in health and disease. Journal of the American College of Cardiology, 63(12), 1111–1119.
- [27] Karimi, K. J. M., Rotich, T. (2025). Mathematical Model for Ions Transport Optimization in an Animal Cell Using MATLAB. International Journal of Mathematical Sciences and Optimization: Theory and Applications, 11(2), 62-73.
- [28] Hall, J. E. (2016). Guyton and Hall Textbook of Medical Physiology, Jordanian Edition E-Book. Elsevier Health Sciences.
- [29] Schultze, A. E. (2007). Book Review: Tietz Textbook of Clinical Chemistry and Molecular Diagnostics. , 129-130
- [30] West, J. B. (2012). Respiratory physiology: the essentials. Lippincott Williams and Wilkins.